

# Effect of storage time on the pressure oxidation enthalpy of pyrite

I. V. Bylina · S. C. Mojumdar · V. G. Papangelakis

CTAS2011 Conference Special Chapter  
© Akadémiai Kiadó, Budapest, Hungary 2012

**Abstract** The information on heat of oxidation–reduction reactions is important for the heat balance and optimization of the autoclave design in the hydrometallurgical industry in ore processing. Pyrite ( $\text{FeS}_2$ ) is a gangue mineral that presents with nickel-containing pentlandite, and copper-containing chalcopyrite minerals. The presence of pyrite impacts to the overall heat of leaching process. This study has been performed on a differential scanning calorimeter (DSC80, Setaram) with a commercial mixing cell to study the thermal behaviour of pure pyrite  $\text{FeS}_2$  (Valdenegrillos, Spain) mineral particles during oxidative pressure leaching at 150 °C and partial oxygen pressure of 3.4 MPa. A calorimetric method for determining the enthalpy of leaching of sulphide minerals at high temperatures and oxygen pressures has been used to evaluate the enthalpies of oxidation of freshly ground pyrite and pyrite stored for a year in contact with air (stored pyrite) under conditions relevant to pressure oxidation operations. Ground pyrite stored over time has long since been known to result in greater heat evolution during oxidative leaching. A likely mechanism for this phenomenon was uncovered: formation of ferrous sulphate and sulphuric acid during storage in contact with air influencing greater heat evolution at the outset of the reaction. Two mass loss steps on TG curve of stored pyrite, attributed to the elimination of atmospheric moisture and  $\text{H}_2\text{O}$  molecule from  $\text{FeSO}_4 \cdot \text{H}_2\text{O}$ , is absent on TG curve of freshly ground pyrite.

**Keywords** DSC · TG · Enthalpy · Pyrite oxidation

## Introduction

The oxidation of freshly ground and stored in the air pyrite ( $\text{FeS}_2$ ) and other sulphide minerals is very important for mining and metallurgical processes. Pyrite is an omnipresent phase in sulphide ore deposits. It is also distributed as a minor phase in a variety of geological settings extending from igneous rocks to sedimentary and hydrothermal deposits [1]. Pyrite weathering is the main process leading to acid mine drainage [2] and results from a combination of oxidation and dissolution processes involving ferric ion and oxygen [3, 4] assisted by microbial activity [5]. In addition, pyrite is a ubiquitous component in the environment and should thus be considered as a reservoir of reductant for toxic oxidized species such as chlorinated compounds and toxic metals. However, the detailed oxidation pathway of pyrite remains partially unknown. Sulphate species are the final stable oxidized sulphur species observed in solution in acidic media.

In hydrometallurgy, pyrite is often associated with refractory gold deposits, or other base metal sulphides requiring processing at high temperatures in acidic solutions, under oxygen pressure (pressure oxidation). This reaction is highly exothermic so that the enthalpy of the reaction is taken into account in designing autoclaves to operate under autothermal conditions, or heat exchange systems to control the reaction temperature [6, 7].

The oxidation of pyrite during storage under normal atmospheric conditions to various hydrated iron sulphates is a known but not well-studied process. The purpose of this study was to evaluate the heats pressure oxidation of freshly ground and stored pyrite by calorimetric measurements.

I. V. Bylina · S. C. Mojumdar · V. G. Papangelakis (✉)  
Department of Chemical Engineering and Applied Chemistry,  
University of Toronto, 200 College Street, Toronto,  
ON M5S 1A4, Canada  
e-mail: vladimirov.papangelakis@utoronto.ca

S. C. Mojumdar  
e-mail: scmojumdar@yahoo.com

These data are important when storage of pyrite and pyrite-containing minerals for long times takes place before processing by pressure oxidation in hydrometallurgical operations. They are also useful for accurate heat balances, optimization of autoclave design, study and modelling of the hydrometallurgical processes.

Thermal analysis and calorimetry are very useful techniques for material characterization and different process studies [8–24]. In this study, we have used XRD, SEM, XPS, ICP-AES and thermal analysis in addition to calorimetry to investigate the oxidative pressure leaching of pyrite. The selection of pyrite was due to its presence in sulphide minerals oxidation processes as well as its relevance in the production of gold. Pyrite can be found in a pure crystalline phase and consequently it is a good reference system.

## Experimental

The enthalpies of oxidative leaching of pyrite were measured using a differential scanning calorimeter (DSC C80, Setaram) equipped with a commercial mixing cell able to operate at temperatures up to 300 °C and pressures up to ~21 MPa. The cell with a nominal volume of 9.1 cm<sup>3</sup> was made from stainless steel and used in combination with a glass liner (4 cm<sup>3</sup> volume) to prevent degradation of the stainless steel cell when working with corrosive mixtures at high temperatures. A schematic diagram of the cell and its inlet and outlet tubes used for gas injection is given in our previous paper [25].

### Pyrite characterization

Natural pyrite (Valdenegrillos, Spain) was purchased from Excalibur Mineral Corp. (USA). The mineral sample was ground in air by a ring mill for ~1 min and dry-sieved to several size fractions. The mineral fraction with the particle size smaller than 37 µm was used for pyrite characterization and for measurements of oxidation enthalpy. A portion of this material was stored, kept in contact with air in a closed plastic tube at room temperature for a period of 1 year. The relative air humidity in the room was 30–60 % during this period.

The chemical analysis of pyrite samples was determined using Inductively Coupled Plasma- Atomic Emission Spectrometry (ICP-AES) on a Perkin Elmer Optima 3000 DV instrument. The phases present in fresh and stored pyrite were identified using powder X-ray diffraction (XRD) on a Philips PW1830 powder X-ray diffractometer. The searchable International Center of Diffraction Data (ICDD), 2005 database was used for identification of the phases in the mineral samples.

XRD analysis showed that fresh pyrite crystals were pure, consisting of only one phase (detection limit ~3–5 wt%).

The pyrite mineral samples also contained trace metals (Ni and Ca) as determined by ICP-AES analysis.

The morphology and purity of fresh pyrite (fraction <37 µm) was investigated using a scanning electron microscope (SEM) with digital imaging capabilities by means of secondary electrons (SE) and backscattered electrons (BSE). The SEM was a JEOL, JSM-840, complemented by a PGT/AAT EDS detector (thin window) and an IXRF 500 digital pulse processor, allowing for X-ray microanalysis and digital imaging via SE, BSE and X-ray signals. The SEM studies (not shown) confirmed that the pyrite sample is pure.

### Chemical analysis

The chemical composition of pyrite samples, solid residues and filtrates was determined by ICP-AES. Mineral samples of 50.0 ± 0.1 mg were digested in 25 mL of boiling aqua regia with continuous agitation for approximately 2–3 h. The resulting solution was then filtered and diluted with deionized water to 250 mL. At the end of the calorimetric measurement, the experimental cell and its contents were cooled down. All unreacted solids remained in contact with the solution for at least 4 h, before being separated at room temperature. After determining the solution pH with a pH-indicator strip (EMD Chemicals Inc., Germany), the slurry was filtered with Fisherbrand filter paper P2. The filtrate was separated and stored. The cell with any remaining residue was rinsed with a mixture of 8 % H<sub>2</sub>SO<sub>4</sub> and 38 % HCl at a volume ratio of 10–1. The solution with residue was heated to 60–70 °C for 2 h under stirring then cooled down, and filtered. The unreacted pyrite and the filter paper were digested in boiling aqua regia (25 mL) before they were analyzed by ICP-AES. The amount of iron sulphate (Fe<sub>2</sub>SO<sub>4</sub>) formed on pyrite surface during pyrite storage in contact with air for 1 year was determined using the following procedure. Since the pyrite is insoluble in hydrochloric acid, about 3 g of stored pyrite was washed with 3 M HCl (100 mL) under heating at about 80 °C for ~2 h. Then, the solution with dissolved FeSO<sub>4</sub> was filtered, diluted with deionized water to 1 L and analyzed by ICP-AES. The amount of FeSO<sub>4</sub> formed on pyrite surface was 18.12 ± 0.17 % of the pyrite mass.

### Enthalpy of oxidative leaching of pyrite

The mineral oxidation was carried out under isothermal conditions. The cell with a weighed amount of mineral (0.0600 ± 0.0002 g) and deionized (Millipore Milli-Q Water System) water (2.0000 ± 0.0002 g) was placed into the calorimeter chamber at room temperature (RT). To expel air from the cell, nitrogen gas was passed through the cell for 20 min at a flow rate of 20.39 ± 0.13 sccm and then the outlet valve of the cell was closed. The mineral

and water were then kept under nitrogen atmosphere at a pressure of 1.4 MPa while heating the cell at a heating rate of 2 °C/min to the final temperature of 150 °C and final pressure of ~2.1 MPa. It took approximately 3–4 h to reach a stable temperature.

Once the temperature was stable to  $\pm 0.02$  °C, oxygen was injected into the cell at a constant flow rate of 10.62 ( $\pm 1.13$  %) up to a partial oxygen pressure of 3.4. Subsequently, the inlet valve of the cell was closed and the system was kept at 150 °C for 10 h since preliminary experiments showed that in some cases up to 8–9 h were required to complete the reaction. After that, the DSC system was cooled down to room temperature with a built-in fan at a rate of 2 °C/min. Cooling was completed in about 4 h. The prolonged period of cooling may cause additional oxidation of the minerals, albeit at progressively slower rates as the temperature drops.

The nitrogen and oxygen flow rates were measured with a Brooks 5850E series controller that was previously calibrated with a portable calibrator Bios Definer 220 ( $\pm 2.2$  %). The pressure was measured with a pressure-sensitive transducer Gefran rated to 35 MPa. A schematic diagram of the experimental setup, calorimeter and injection system is presented in [25].

The performance of the DSC was first evaluated by measuring the enthalpy of dissolution of potassium chloride salt (Standard Reference Material 1655, the National Institute of Standards and Technology) in water at 25 °C [26–28]. The measured enthalpy of dissolution of KCl,  $17.25 \pm 0.01$  kJ mol<sup>-1</sup> ( $\pm 0.06$  %) was found to be in excellent agreement with the literature value of 17.22 kJ mol<sup>-1</sup> [29].

### Enthalpy calculations

The overall enthalpy change,  $\Delta H_{\text{exp}}$ , was obtained by integration of the DSC curve as a function of time. The measured enthalpy includes: (i) the heat of oxidation-dissolution of the mineral,  $\Delta H_{\text{oxid}}(\text{mineral})$ ; (ii) the heat of dissolution of oxygen in water,  $\Delta H_{\text{diss}}(\text{O}_2)$ ; (iii) and the heat required for raising the oxygen temperature from room temperature to 150 °C,  $\Delta H_{\text{heat}}(\text{O}_2)$ . The following equation describes the relationship.

$$\Delta H_{\text{exp}} = \Delta H_{\text{oxid}}(\text{mineral}) + \Delta H_{\text{diss}}(\text{O}_2) + \Delta H_{\text{heat}}(\text{O}_2) \quad (1)$$

To determine the contributions of the  $\Delta H_{\text{diss}}(\text{O}_2)$  and  $\Delta H_{\text{heat}}(\text{O}_2)$  to the overall experimental enthalpy, blank experiments were carried out. The  $\Delta H_{\text{blank}} = \Delta H_{\text{diss}}(\text{O}_2) + \Delta H_{\text{heat}}(\text{O}_2)$  was obtained from a run with water and oxygen without mineral charge, under the same conditions used for the actual experiments. The heat of mineral oxidation was then estimated using Eq. 2. The Setsoft 2000 software distributed by Setaram was used for this estimation.

$$\Delta H_{\text{oxid}}(\text{mineral}) = \Delta H_{\text{exp}} - \Delta H_{\text{blank}} \quad (2)$$

### XPS analysis of pyrite surface

The chemical analysis of the freshly ground pyrite and stored pyrite were also determined by X-ray photoelectron spectroscopy (XPS). XPS data were obtained with monochromatic AlK $\alpha$  X-ray source radiation. The pyrite samples with particle size <37  $\mu\text{m}$ , prepared as described above were used for surface studies.

### TG–DSC analysis

Thermogravimetric–differential scanning calorimetric analysis (TG–DSC) was also carried out using a simultaneous differential thermal analyzer, SDT Q600 (TA Instruments). Measurements were conducted under nitrogen atmosphere (purity 99.9999 %) at a flow rate of 100 mL/min. Samples with particles size <37  $\mu\text{m}$ , having a mass of about 25 mg, were placed in a platinum crucible and heated at a linear heating rate of 10 °C/min over a temperature range from ambient to 700 °C. Replicate measurements for freshly ground pyrite showed good reproducibility: the standard deviation of weight loss and peak temperature was  $\pm 1.25$  % and  $\pm 3.53$  °C, respectively.

## Results and discussion

### Heat of oxidative pressure leaching of freshly ground pyrite

The amount of unreacted pyrite in the solid residue must be known to determine the molar heat of reaction. However, the very small reactor volume made the recovery of the samples very difficult and some approximations had to be made in order to estimate the degree of conversion from mineral to products.

The XRD analysis of the residue after pyrite oxidation showed significant amount of unreacted pyrite. The XRD patterns of the original mineral and the solid products were identical. The amount of unreacted pyrite in the solid residue was estimated from the sulphur content in the residue after aqua regia digestion using Eq. (3) and the moles of haematite formed—using Eq. (4).

$$\text{mol}(\text{FeS}_2)_{\text{unreacted}} = \text{mol} S_{\text{residue}}/2 \quad (3)$$

$$\text{mol} \text{Fe}_2\text{O}_3 = [\text{mol} \text{Fe}_{\text{residue}} - (\text{mol} S_{\text{residue}}/2)]/2 \quad (4)$$

Table 1 summarizes the results and presents the enthalpy values for pyrite oxidation. The average molar enthalpy value at  $P_{\text{O}_2}$  of 3.4 MPa is  $\Delta H_{\text{av}} = -512 \pm 12$  kJ mol<sup>-1</sup>

**Table 1** Oxidation enthalpy of freshly ground pyrite at 150 °C and  $P_{O_2}$  of 3.4 MPa

| Mineral mass/mg | Reacted FeS <sub>2</sub> /mg | Reacted FeS <sub>2</sub> /% | Net heat of reaction/J | Molar heat of reaction/kJ/mol | Specific heat of reaction/kJ/kg |
|-----------------|------------------------------|-----------------------------|------------------------|-------------------------------|---------------------------------|
| 60.1            | 13.5                         | 22                          | -57.51                 | -513                          | -4272                           |
| 60.1            | 14.5                         | 24                          | -60.23                 | -499                          | -4161                           |
| 60.1            | 13.6                         | 23                          | -59.27                 | -523                          | -4358                           |

with standard deviation 2.34 %. Because of the small amount of the samples, filtrates and residues, the ratio of sulphate to elemental sulphur formed and the ratio of ferrous to ferric irons could not be determined with sufficient accuracy. This analysis would have enabled us to know the exact extent of chemical reactions occurring between FeS<sub>2</sub> and O<sub>2</sub>.

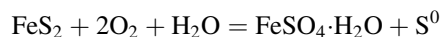
If we assume that all sulphur from pyrite is oxidized to sulphate and all iron oxidized to Fe(III), the heat of the overall reaction, evaluated with the HSC Chemistry 5.0 software, would be -1655 kJ/mol FeS<sub>2</sub>. In this case, the estimated enthalpy (-1655 kJ/mol) is 3.2 times higher than the average experimental value of  $-512 \pm 12$  kJ/mol at  $P_{O_2}$  of 3.4 MPa (Table 1). However, if we assume that all sulphur from pyrite is converted to elemental sulphur and all iron oxidizes to Fe(III), then the overall heat of reaction would be -306 kJ/mol FeS<sub>2</sub>. This value is closer to the experimental enthalpy  $-512 \pm 12$  kJ/mol at a partial oxygen pressure of 3.4 MPa (Table 1), suggesting that pyrite oxidation under these conditions mainly proceeded to elemental sulphur. The fact that the reaction did not proceed to completion is likely because of O<sub>2</sub> transfer limitations.

#### Effect of pyrite storage on its oxidation enthalpy

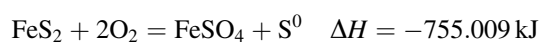
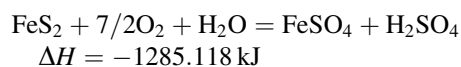
The enthalpies of pyrite oxidation at 150 °C under high oxygen pressure (3.4 MPa) are different between freshly ground pyrite (Table 1) and stored pyrite (Table 2). We believe that the reason for such difference (Fig. 1) is that the oxidation of stored pyrite proceeds to sulphate formation more than the freshly ground pyrite. It is possible that

the formation of iron sulphates on the particles surface when pyrite is kept under storage catalyzes this reaction by providing higher amounts of iron in solution. The amount of FeSO<sub>4</sub>·H<sub>2</sub>O in the stored pyrite identified by chemical analysis was 18.12 %.

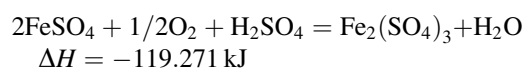
The proposed reaction of iron sulphate formation on pyrite surface is as follows:



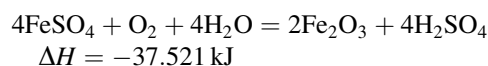
The pyrite oxidation is described by the following reactions with their heat values at 150 °C as evaluated by the HSC software. Oxidation of pyrite by oxygen with formation of Fe<sup>2+</sup>:



In acidic conditions Fe<sup>2+</sup> is oxidized by oxygen to Fe<sup>3+</sup>:



This reaction is limited by the rate of oxygen diffusion into the pyrite surface. Fe<sup>3+</sup> is the preferred oxidizing agent over oxygen. Once Fe<sup>3+</sup> is formed, contribution of O<sub>2</sub> to direct pyrite oxidation becomes minimal; it is this Fe(III) that likely plays a role to the production of SO<sub>4</sub> rather than S<sup>0</sup>, and ultimately responsible for the observed higher oxidation enthalpy values. Fe<sup>2+</sup> oxidation to Fe<sup>3+</sup> is quickly followed by hydrolysis to Fe(III) oxide (haematite). In this case, the overall reaction enthalpy is considerably less.



#### XRD and XPS analysis for freshly ground and stored pyrite

The XRD analysis of fresh and stored pyrites showed the difference. Thus, the freshly ground pyrite crystals are pure and only one phase presents. In the case of stored pyrite, the second phase of iron sulphate monohydrate, FeSO<sub>4</sub>·H<sub>2</sub>O, or Szomolnokite was identified by the XRD analysis. It was suspected that the difference in heat

**Table 2** Enthalpy of oxidation of stored pyrite at 150 °C and  $P_{O_2}$  of 3.4 MPa

| Mineral mass/mg | Pyrite amount/mg | Reacted FeS <sub>2</sub> /mg | Reacted FeS <sub>2</sub> /% | Reacted FeS <sub>2</sub> /mol × 10 <sup>-4</sup> | Heat of reaction/J | Molar heat of reaction/kJ/mol | Specific heat of reaction/kJ/kg |
|-----------------|------------------|------------------------------|-----------------------------|--|--------------------|-------------------------------|---------------------------------|
| 59.9            | 49.12            | 28.9                         | 48                          | 2.42   | -181.15            | -750                          | -6249                           |
| 60.0            | 49.20            | 30.9                         | 52                          | 2.58   | -188.0             | -730                          | -6084                           |
| 60.0            | 49.20            | 29.5                         | 49                          | 2.46   | -186.79            | -760                          | -6338                           |

$\Delta H_{av} = -747 \pm 15$  kJ/mol ( $\pm 2.07$  %) or  $-6224 \pm 129$  kJ/kg ( $\pm 2.07$  %)

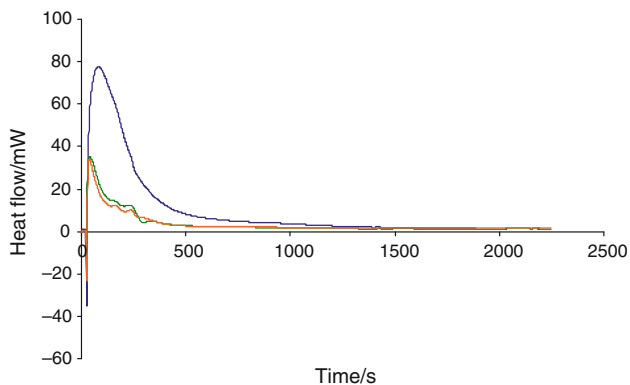


**Fig. 1** DSC curves of oxidation of freshly ground (*bottom two curves*) and stored pyrite (*top and intensive curve*)

evolution between freshly ground and stored pyrite was due to chemical changes taking place in the mineral.

The XPS analysis results at room temperature showed that the freshly ground pyrite contains only iron sulphide whereas the stored pyrite consists of sulphides and sulphates.

**Thermal analysis results**

TG and DSC curves of freshly ground and stored pyrite are given in Figs. 2 and 3, respectively. There are big differences on the TG and DSC curves of freshly ground and stored pyrite up to 350 °C. There is no significant mass loss and DSC peak on TG and DSC curves, respectively, of

**Fig. 2** TG and DSC curves of freshly ground pyrite at heating rate of 10 °C/min

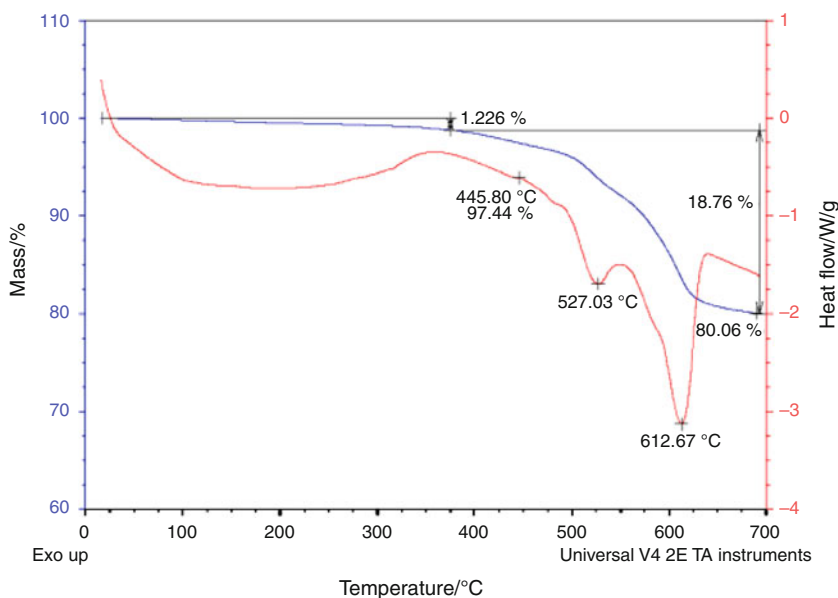
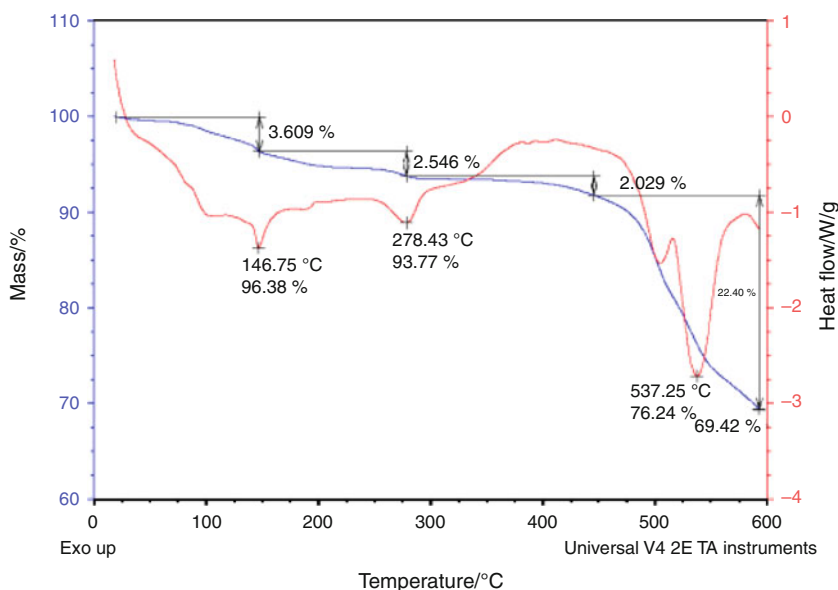


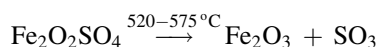
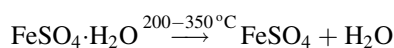
**Fig. 3** TG and DSC curves of stored pyrite at heating rate of 10 °C/min





freshly ground pyrite till 350 °C. However, two significant mass loss steps on TG curve of stored pyrite at room temperature –200 °C and 200–350 °C have been observed with the corresponding endothermic DSC peaks. These two mass loss steps are attributed to the elimination of atmospheric moisture and H<sub>2</sub>O molecule from FeSO<sub>4</sub>·H<sub>2</sub>O. The thermal behaviour of freshly ground and stored pyrite does not have big difference after 350 °C. The TG curves for both pyrites are accompanied by a mass loss step at 350–520 °C (Figs. 2, 3) and attributed to the elimination of SO<sub>2</sub>. The TG curves for both pyrites exhibit another mass loss step at 520–575 °C (Figs. 2, 3) and attributed to the elimination of SO<sub>3</sub> with the simultaneous formation of Fe<sub>2</sub>O<sub>3</sub>.

Thermal decomposition of FeSO<sub>4</sub>·H<sub>2</sub>O, main pyrite oxidation product can be represented as:



## Conclusions

- The measured enthalpy for stored pyrite oxidation at 150 °C,  $-187 \pm 5$  J is  $\sim 3.4$  times more exothermic than that of freshly ground pyrite  $-55 \pm 3$  J
- The difference in enthalpies was explained by formation of iron sulphate monohydrate and sulphuric acid on the pyrite surface during its storage for 1 year in contact with moist air. The XRD analysis identified the second phase of FeSO<sub>4</sub>·H<sub>2</sub>O (Szomolnokite) in stored pyrite. The chemical analysis identified this phase to be  $\sim 18$  % of the mineral mass. The formation of ferrous sulphate and sulphuric acid during storage in contact with moist air influencing greater heat evolution at the outset of the reaction
- The extra iron on the surface oxidizes by oxygen to Fe(III) and contributes to promoting the oxidation of pyrite to sulphate, rather than elemental sulphur, which is a more exothermic reaction. The results in higher exothermicity for stored pyrite oxidation compared to freshly ground pyrite.
- Two significant mass loss steps on TG curve of stored pyrite at RT–200 °C and 200–350 °C, attributed to the elimination of atmospheric moisture and H<sub>2</sub>O molecule from FeSO<sub>4</sub>·H<sub>2</sub>O is absent on TG curve of freshly ground pyrite.

**Acknowledgements** This study has been financially supported by Natural Science and Engineering Research Council (NSERC) and Vale. The acquiring and interpreting of the XRD, SEM and XPS

analysis results, provided by George Kretschmann (Geology) and Peter Brodersen (SIO, Chemical Engineering and Applied Chemistry Department) at the University of Toronto are gratefully acknowledged.

## References

1. Xiao Z, Chen Q, Yin Z, Hu H, Zhang P. Calorimetric studies on leaching of mechanically activated sphalerite in FeCl<sub>3</sub> solution. *Thermochim Acta*. 2004;416:5–9.
2. Gao WY, Wang YW, Dong LM, Yu ZW. Thermokinetic analysis of the hydration process of calcium phosphate cement. *J Therm Anal Calorim*. 2006;85:785–9.
3. Aukett PN, Bensted J. Application of heat flow calorimetry to the study of oil well cements. *J Therm Anal Calorim*. 1992;38:701–7.
4. Mathonat C, Hypek V, Majer V, Grolier J-PE. Measurements of excess enthalpies at high temperature and pressure using a new type of mixing unit. *J Solution Chem*. 1994;23:1161–82.
5. Koschel D, Coxam J-Y, Majer V. Enthalpy and solubility data of H<sub>2</sub>S in water at conditions of interest for geological sequestration. *Ind Eng Chem Res*. 2007;46:1421–30.
6. Papangelakis VG, Demopoulos GP. Aqueous pressure oxidation of pyrite: reaction kinetics. *Hydrometallurgy*. 1991;26:309–25.
7. Papangelakis VG, Demopoulos GP. On the attainment of stable autothermal operation in continuous pressure leaching reactor. *Hydrometallurgy*. 1992;29:297–318.
8. Masson J-F, Bundalo-Perc S. Calculation of smoothing factors for the comparison of DSC results. *J Therm Anal Calorim*. 2007; 90:639–43.
9. Chowdhury B, Mojumdar SC. Aspects of thermal conductivity relative to heat flow. *J Therm Anal Calorim*. 2005;81:179–82.
10. Simon P, Illekova E, Mojumdar SC. Kinetics of crystallization of metallic glasses studied by non-isothermal and isothermal DSC. *J Therm Anal Calorim*. 2006;83:67–9.
11. Mojumdar SC, Sain M, Prasad R, Sun L, Venart JES. Selected thermoanalytical methods and their applications from medicine to construction: part I. *J Therm Anal Calorim*. 2007;90:653–62.
12. Jingyan S, Yuwen L, Jie L, Zhiyong W, Cunxin W. Calorimetry studies of a chemical oscillatory system: the effect of putrescine on KSCN–H<sub>2</sub>O<sub>2</sub>–CuSO<sub>4</sub>–NaOH reactions. *J Therm Anal Calorim*. 2007;90:761–7.
13. Pajtášová M, Ondrušová D, Jóna E, Mojumdar SC, Ľalíková S, Bazyláková T, Gregor M. Spectral and thermal characteristics of Copper(II) carboxylates with fatty acid chains and their benzothiazole adducts. *J Therm Anal Calorim*. 2010;100:769–77.
14. Gonsalves LR, Mojumdar SC, Verenkar VMS. Synthesis and characterisation of Co<sub>0.8</sub>Zn<sub>0.2</sub>Fe<sub>2</sub>O<sub>4</sub> nanoparticles. *J Therm Anal Calorim*. 2011;104:869–73.
15. Rejitha KS, Mathew S. Investigations on the thermal behavior of hexaamminenickel(II) sulphate using TG-MS and TR-XRD. *Glob J Anal Chem*. 2010;1(1):100–8.
16. Drebuschak VA, Turkin AI. Changes in the heat capacity of Al<sub>2</sub>O<sub>3</sub>–Cr<sub>2</sub>O<sub>3</sub> solid solutions near the point of antiferromagnetic phase transition in Cr<sub>2</sub>O<sub>3</sub>. *J Therm Anal Calorim*. 2007;90:795–9.
17. Janotka I, Mojumdar SC. Degree of hydration in cement paste and C3A–sodium carbonate–water systems. *J Therm Anal Calorim*. 2007;90:645–52.
18. Dovál M, Palou M, Mojumdar SC. Hydration behavior of C2S and C2AS nanomaterials synthesized by sol–gel method. *J Therm Anal Calorim*. 2006;86:595–9.
19. Mojumdar SC, Raki L. Preparation, thermal, spectral and microscopic studies of calcium silicate hydrate–poly(acrylic acid) nanocomposite materials. *J Therm Anal Calorim*. 2006;85: 99–105.

20. Vourlias G, Pistofidis N, Chrissafis K, Stergioudis G. Zinc coatings for oxidation protection of ferrous substrates: part I. Macroscopic examination of the coating oxidation. *J Therm Anal Calorim.* 2007;90:769–75.
21. Raileanu M, Todan L, Crisan M, Braileanu A, Rusu A, Bradu C, Carpov A, Zaharescu M. Sol–gel materials with pesticide delivery properties. *J Environ Prot.* 2010;1:302–13.
22. Mojumdar SC, Mazanec K, Drabik M. Macro-defect-free (MDF) cements. *J Therm Anal Calorim.* 2006;83:135–9.
23. Vourlias G, Pistofidis N, Pavlidou E, Chrissafis K. Zinc coatings for oxidation protection of ferrous substrates: part II. Microscopic and oxidation mechanism examination. *J Therm Anal Calorim.* 2007;90:777–82.
24. Mojumdar SC, Moresoli C, Simon LC, Legge RL. Edible wheat gluten (WG) protein films: preparation, thermal, mechanical and spectral properties. *J Therm Anal Calorim.* 2011;104:929–36.
25. Bylina I, Trevani L, Mojumdar SC, Tremaine P, Papangelakis VG. Measurement of reaction enthalpy during pressure oxidation of sulphide minerals. *J Therm Anal Calorim.* 2009;96:117–24.
26. Nesterenko VP. Thermodynamic investigation of zirconium diselenite. *J Therm Anal Calorim.* 2005;80:575–7.
27. Archer DG. Thermodynamic properties of the KCl + H<sub>2</sub>O system. *J Phys Chem Ref Data.* 1999;28:1–17.
28. Zhang ZH, Ku ZJ, Li HR, Liu Y, Qu SS. Calorimetric and thermal decomposition kinetic study of Tb(Tyr)(Gly)<sub>3</sub>Cl<sub>3</sub>·3H<sub>2</sub>O. *J Therm Anal Calorim.* 2005;79:169–73.
29. Parker VB. Thermal properties of uni-univalent electrolytes. National Standard Reference Data Series—National Bureau of Standards. In: Lide DR Editor-in-Chief. *Handbook of chemistry and physics*, 79th ed. Boca Raton: CRC; 1998–1999. p. 5–103.